

Metformin promotes the normalization of abnormal blood vessels after radiofrequency ablation deficiency in hepatocellular carcinoma by microRNA-302b-3p targeting thioredoxin-interacting protein

HaiGang Niu^{1,2}, ShuYing Dong¹, GuoMing Li³, ShiLun Wu¹ and WenBing Sun¹✉

¹Department of Hepatobiliary Surgery, Beijing Chaoyang Hospital Affiliated to Capital Medical University, Beijing, 100043, China; ²Department of Clinical Medicine, Fenyang College of Shanxi Medical University, Fenyang, Shanxi Province, 032200, China; ³The Second Department of General Surgery, Chaoyang Central Hospital, Chaoyang, Liaoning Province, 122000, China

Metformin has shown great promise in the treatment of HCC. Radiofrequency ablation (RFA) deficiency results in recurrence and metastasis of remaining HCC tumors. Here, we aimed to investigate the role and mechanism of metformin in HCC after RFA deficiency. HCC cell line Hep-G2 was selected to simulate RFA deficiency and named HepG2-H cells. After treating cells with different concentrations of metformin (2.5, 5, 10 μ M) or transfecting related plasmids, cell proliferation, migration, invasion, apoptosis and angiogenesis were detected, *in vitro* permeability test was performed, and an angiogenesis-related protein VEGFA was analyzed. The residual HCC model after RFA deficiency was established in mice. Metformin was administered by gavage to detect changes in tumor volume and weight, and CD31 staining was used to observe microvessels. The targeting relationship between miR-302b-3p and *TXNIP* was demonstrated by the bioinformatics website, dual-luciferase reporter assay, and RNA pull-down assay. The results found that metformin inhibited RFA deficiency-induced growth and angiogenesis of HCC cells *in vitro*. miR-302b-3p counteracted the therapeutic effect of metformin on RFA deficiency. miR-302b-3p targeted regulation of *TXNIP*. The up-regulation of *TXNIP* reversed the effects of over-expression of miR-302b-3p on RFA-deficient HCC cells. Metformin inhibited RFA-deficiency-induced HCC growth and tumor vascular abnormalities *in vivo*. Overall, metformin promotes the normalization of abnormal blood vessels after RFA deficiency in HCC by miR-302b-3p targeting *TXNIP*, which can be used to prevent the progression of HCC after RFA.

Keywords: Metformin; radiofrequency ablation deficiency; MicroRNA-302b-3p; Thioredoxin-interacting protein

Received: 29 March, 2022; revised: 22 August, 2022; accepted: 04 February, 2023; available on-line: 22 December, 2023

✉ e-mail: sunwb_swb440@outlook.com

Abbreviations: HCC, Hepatocellular carcinoma; miRNAs, microRNAs; RFA, Radiofrequency ablation; UTR, 3'-untranslated region

INTRODUCTION

Hepatocellular carcinoma (HCC) is an extremely familiar primary liver malignancy and the main reason for cancer-linked deaths worldwide (Harati *et al.*, 2021). Over the past 10 years, the incidence of HCC has been increasing, causing a huge socioeconomic burden (Schulte *et al.*, 2019). Because the early symptoms of HCC are

ambiguous, most patients are already at an advanced stage when being diagnosed, and are accompanied by distant tumor metastasis, leading to an extremely unpleasing overall survival rate and prognosis (El Shorbagy *et al.*, 2021). Currently, the clinical approaches for HCC mainly cover surgical resection, chemotherapy, drug therapy, and surgical resection. However, not all patients can undergo surgical resection, and there are few effective options for patients at an advanced stage. Radiofrequency ablation (RFA) has been successfully applied to treat diversified primary tumors, covering HCC (Lassandro *et al.*, 2020). However, the malignant progression of residual HCC cells after RFA limits the treatment outcome of patients (Jia *et al.*, 2020).

Metformin is anti-tumor (Shankaraiah *et al.*, 2019) and it can restrain the malignant progression of HCC through multiple signaling pathways. For example, metformin refrains liver cancer cell proliferation by reducing the glycolytic flux of the hypoxia inducible factor (HIF)-1 α /6-phosphofructo-2-kinase/fructose-2,6-bisphosphatase 3/phosphofructokinase-1 pathway (Hu *et al.*, 2019). Metformin represses HCC progression by activating the Hippo pathway (Zhao *et al.*, 2021). Meanwhile, metformin synergizes with other drugs to refrain the progression and the drug resistance of HCC. For example, metformin combined with curcumin refrains HCC growth, metastasis, and angiogenesis *in vitro* and *in vivo* (Zhang *et al.*, 2018). Metformin can enhance the sensitivity of orthotopic HCC mice to sorafenib, thereby decreasing postoperative recurrence and metastasis of HCC (You *et al.*, 2016). However, the role of metformin in HCC after RFA is uncertain.

MicroRNAs (miRNAs) are a class of short endogenous single-stranded non-coding RNAs that reduce mRNA stability and translation by combining with the 3'-untranslated region (UTR) of target mRNAs (Alberti *et al.*, 2018). Plentiful studies have manifested that abnormal expression of miRNAs is linked with the occurrence of cancers covering HCC (Yerukala *et al.*, 2020). For example, miR-15a-3p represses HCC metastasis by interacting with heme oxygenase 1 (Jiang *et al.*, 2020) and miR-448 depresses cell growth by targeting B cell lymphoma 2 in HCC (Liao *et al.*, 2019). MiR-302b-3p is a pluripotency-linked miRNA, which has been discovered to participate in the physiological and pathological processes of cancers, such as pancreatic cancer (Xu *et al.*, 2021), gastric cancer (Wang *et al.*, 2021), and colorectal cancer (Hu *et al.*, 2021). However, no study has indicated its expression and function in HCC.

This study aimed to investigate the function and latent mechanisms of metformin in HCC after RFA deficiency. *In vivo* and *in vitro* experiments were conducted to determine the function of metformin in the growth and angiogenesis of residual HCC cells after RFA deficiency, and further analyze the interaction between metformin and miR-302b-3p. It is hypothesized that metformin promotes the normalization of abnormal blood vessels after HCC by miR-302b-3p targeting the thioredoxin-interacting protein, offering new insights into HCC treatment.

MATERIALS AND METHODS

Tissue sample

Human HCC tissue and para-tumor samples were collected from 45 HCC patients who underwent surgical resection, while 18 of them were residual tumors from RFA-undertreated HCC patients. All tissue samples were kept in liquid nitrogen at -80°C , and informed consent was obtained and approved by the Ethics Committee of our hospital.

Cell culture

HCC cell line Hep-G2 (Type Culture Bank of the Chinese Academy of Sciences, Shanghai, China) and normal human liver cell line L02 (Shanghai Academy of Sciences, Shanghai) were cultured with 10% fetal bovine serum, 100 U/mL penicillin, and 100 mg/mL streptomycin in Roswell Park Memorial Institute-1640 medium (Gibco) (Ni *et al.*, 2021). All the media were provided by Gibco.

In vitro RFA deficiency

RFA deficiency was modeled *in vitro* as previously described (Zhang *et al.*, 2017). Briefly, Hep-G2 cells were seeded in 6-well plates (5×10^4 cells/well) and immersed in water at 47°C after 24 h. Afterward, cells were allowed to recover, and when the surviving cells reached 80% confluence, cells were propagated into 6-well plates and treated for 10 min as described above. This process was repeated ten times for 15, 20, and 25 min in sequence. Cells that survived were named HepG2-H cells.

Cell transfection

The pcDNA3.1 (+) vector for *TXNIP* overexpression and its corresponding control, miR-302b-3p mimic, miR-302b-3p inhibitor, and their negative controls were all synthesized by GenePharma (Shanghai, China). Cells were seeded in 6-well plates at a density of 5×10^5 cells/well and transfected after 24 h of incubation. *In vitro* transfection was performed using LipofectamineTM 3000 reagent (Thermo Fisher Scientific).

Cell viability

A total of 5×10^3 cells were seeded and incubated in 96-well plates. Then, 10 μL CCK-8 solution (CCK-8, Dojindo, Tokyo, Japan) was added to each well. Finally, the absorbance was read at 450 nm (Zhang *et al.*, 2021).

Colony formation assay

Cells were plated in 6-well plates at 500 cells/well. The colonies formed on the plate were fixed with 4% paraformaldehyde (Solabio), stained with 0.5% crystal violet, and counted (Zhu *et al.*, 2019).

2Transwell assay

Cells were made into cell suspension at $1 \times 10^6/\text{mL}$. In the invasion assay, 50 mg/L Matrigel was diluted at a ratio of 1: 8 and spread on the bottom of the chamber. Matrigel was not applied in the migration assay. Then, 600 μL complete medium was added to the lower chamber and 200 μL cell suspension was placed in the bottom chamber. After 24 h, the chamber was washed with phosphate-buffered saline (PBS), and the cells were fixed with paraformaldehyde (40 g/L) and stained with crystal violet (1 g/L). Finally, cells were counted under an inverted microscope in 6 fields of view (Xu *et al.*, 2021).

Apoptosis detection

Apoptosis assays were performed with Alexa Fluor 488-Annexin V/propidium iodide (PI) (Invitrogen, CA, USA). A BD LSR II flow cytometer (BD Biosciences, San Jose, CA, USA) was utilized to acquire the data and FlowJo analysis software (Tree Star, Inc., Ashland, OR, USA) was used to evaluate the results. Annexin V positive cells were regarded as apoptotic cells.

Tube formation experiment

A conditioned medium of tumor cells was collected. Afterward, 2×10^4 human umbilical vein endothelial cells (HUVECs) were incubated with 100 μL conditioned medium and observed with an inverted microscope (CKX40, Olympus). The branch point numbers were counted in 5 random fields.

In vitro permeability assay

HUVECs were plated on transwell membranes (0.4 μm in diameter; Corning-Costar, New York, USA). Subsequently, rhodamine-dextran (average MW $\sim 70,000$; 20 mg/ml) was added to the upper chamber. The absorption of 40 μL the lower cavity medium was measured at 544 nm excitation wavelength and 590 nm emission wavelength.

Quantitative real-time polymerase chain reaction (PCR)

Extraction of total RNA was done using Trizol (15596-018, Invitrogen). cDNA was synthesized from 1 μg RNA by cDNA Synthesis Kit (K1631, Thermo Fisher Scientific). In a PCR detection system (CFX96, Bio-Rad, Hercules, CA, USA), PCR reactions were performed with the One-step PrimeScript RT-PCR kit (RR064B, Takara, Shiga, Japan). The thermal protocol was set as pre-denaturation at 95°C for 5 min, denaturation at 95°C for 15 s, annealing at 58°C for 30 s, extension at 72°C for 30 s, for a total of 40 cycles, and extension at 72°C for 10 min. Glyceraldehyde-3-phosphate dehydrogenase (GAPDH) and $\beta\text{-actin}$ were internal controls. The primer sequences were manifested in Table 1. Relative expression was analyzed by the $2^{-\Delta\Delta\text{CT}}$ method (Teng *et al.*, 2020).

Western blot

Cells were lysed by a mixture of protease inhibitor and radio-immunoprecipitation assay lysis buffer. Protein samples were separated by 10% sodium dodecyl sulfate-polyacrylamide gel electrophoresis and then electro-blotted onto polyvinylidene fluoride (PVDF) membranes (Bio-Rad). After blocking with 5% skim milk powder, the PVDF membranes were incubated with anti-human *TXNIP* (ab188865, 1: 1000, Abcam), vascular endothelial growth factor A (ab46154, VEGFA; 1: 1000, Abcam),

Table 1 Primer sequence

Genes		Primer sequence (5'-3')
miR-302b-3p	Human	ACACTCCAGCTGGGTAAGTGCTCCATGTTT
		TGGTGTCTGGAGTCG
	mouse	ACACTCCAGCTGGGTAAGTGCTCCATGTTT
		TGGTGTCTGGAGTCG
TXNIP	Human	GGTCTTTAACGACCCTGAAAAGG
		ACACGAGTAACCTCACACACCT
	mouse	GGCCGGACGGTAATAGTG
		AGCGCAAGTAGTCCAAAGTCT
U6	Human	CTCGCTTCGGCAGCACA
		AACGCTTCACGAATTTGCGT
	mouse	CTCGCTTCGGCAGCACA
		AACGCTTCACGAATTTGCGT
GAPDH	Human	GGAGCGAGATCCCTCCAAAAT
		GGCTGTTGCATACTTCTCATGG
	mouse	ATCACTGCCACCCAGAAG
		ATCACTGCCACCCAGAAG
Genes		Primer sequence (5'-3')
MiR-302b-3p		F: 5'-GCGTAAGTGCTCCATGTT-3'
		R: 5'-TCCAGGGACCGAGGA-3'
TXNIP		F: 5'-CGCTCCTGCTTGAACTA-AC-3'
		R: 5'-AATATACGCCGCTGGTTACACT-3'
U6		F: 5'-CTCGCTTCGGCAGCACA-3'
		R: 5'-AACGCTTCACGAATTTGCGT-3'
GAPDH		F: 5'-CGCTCTGCTCCTCCTGTTT-3'
		R: 5'-ATCCGTTGACTCCGACCTTCAC-3'

Note: F, forward; R, reverse.

and GAPDH (2118, 1: 1000, Cell Signaling Technology). Proteins were developed by a chemiluminescence detection system (Millipore, MA, USA) and imaged by a FluroChem E imager (Protein Simple, Santa Clara, CA, USA) (Sun *et al.*, 2021). Densitometry and quantification were performed using Image Lab™ software (version 3.0) (Bio-Rad Laboratories).

The luciferase activity assay

The target genes of miR-302b-3p were predicted by Starbase 3.0. The wild-type (Wt) or mutant (Mut) sequence of *TXNIP* was cloned into the dual-luciferase reporter vector pGL3. The reporter was then co-transfected with miR-302b-3p mimic or NC into HepG2-H cells using Lipofectamine 2000 (Invitrogen). The relative luciferase activity was determined in the light of the instructions of the dual luciferase reporter kit (Promega) (Yuan *et al.*, 2020).

RNA pull-down analysis

HepG2-H cells were transfected with biotinylated miR-302b-3p (Bio-miR-302b-3p) and biotinylated NC (Bio-NC) (RiboBio). Then, cells were lysed and incu-

bated with streptavidin beads (Thermo Fisher Scientific). Afterwards, the bound RNA was eluted and purified using the RNeasy Mini Kit (Qiagen) and analyzed by PCR to measure *TXNIP* expression.

Tumors in nude mice

Twelve male BALB/c nude mice (nu/nu) (6 weeks old; body weight of 16–20 g) were purchased from the Model Animal Research Center of Nanjing University. The mice were raised in cages (n=6/cage) and placed in a sterile room with 12-h light/dark cycle with free access to food and water. All animal studies complied with the regulations of the Institutional Animal Care and Use Committee and were approved by the Medical Ethics Committee of Beijing ChaoYang Hospital, Capital Medical University. HepG2-H cells (5×10^6) were suspended in 200 μ l serum-free Dulbecco's Modified Eagle Medium and Matrigel (1:1) and injected subcutaneously in the upper right flank. After 1 week, mice were orally administered metformin (200 mg/kg/d) or PBS as a control for 24 d. The size of the xenograft tumor was measured with a vernier caliper every 6 d, and the tumor volume was calculated according to the formula of

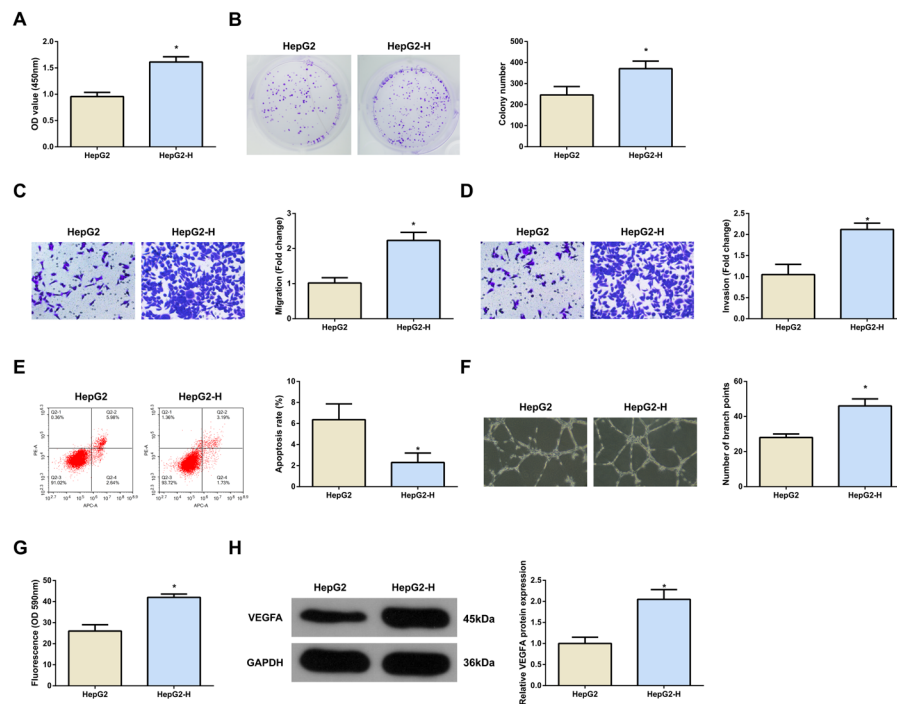


Figure 1. RFA promotes HCC cell growth and tumor angiogenesis

After RFA treatment, (A) CCK-8 detection of cell viability; (B) Plate clone detection of cell proliferation; (C/D) Transwell detection of cell migration and invasion; (E) Flow cytometry detection of cell apoptosis; (F) Detection of angiogenesis; (G) Permeability assay *in vitro*. (H) Western blot detection of angiogenesis-linked protein VEGFA. N=3. The measurement data were presented as mean \pm S.D. *vs. the HepG2, $P < 0.05$.

$0.5 \times \text{length} \times \text{width}^2$. After 24 d, the mice were euthanized by cervical dislocation, and tumor tissues were collected for pathological and molecular expression analysis.

CD31 immunohistochemistry

Tumor tissue was fixed and embedded in paraffin. The tumor sections (5 μm) were incubated with a rabbit monoclonal antibody CD31 (550274, eBioscience, Inc., San Diego, CA, USA) or the universal NC antibody control. After incubation with the appropriate biotinylated secondary antibody, the sections were incubated with horseradish peroxidase-conjugated streptavidin (KeyGen Biotech.), followed by the addition of 3,3'-diaminobenzidine working solution (Sigma) and counterstaining with hematoxylin. Quantification of intratumoral microvessel density (IMVD) was performed by counting CD31-positive (brown) cells in the nine most vascularized areas.

Statistical analysis

Data were analyzed with SPSS (IBM, Armonk, NY, USA) and manifested as mean \pm standard deviation (S.D.). Differences were analyzed by Student's *t*-test or one-way analysis of variance (ANOVA) and Tukey's post-hoc test. Correlation analysis was done with Pearson analysis. $P < 0.05$ emphasized statistical meaning.

RESULTS

This study explored the potential role and mechanism of metformin in RFA deficiency of HCC. *In vivo* and *in vitro* experiments were performed to determine the function of metformin in the cell growth and angiogenesis of HCC after RFA deficiency, and the interaction between

metformin and miR-302b-3p was further analyzed. It is concluded that metformin promotes the normalization of abnormal blood vessels after RFA deficiency in HCC by miR-302b-3p targeting *TXNIP*, which can be used to prevent the progression of HCC after RFA.

RFA promotes the growth of HCC cells and accelerates tumor angiogenesis

To study the impact of metformin on RFA-deficient HCC cells, RFA deficiency *in vitro* was simulated to construct a cell model named HepG2-H. As measured, the proliferation, invasion, and migration were promoted and apoptosis was reduced in HepG2-H cells after RFA (Fig. 1A–E). Angiogenesis, the process by which original blood vessels grow out of new blood vessels, has been implicated in the growth and progression of solid tumors (Ramjiawan *et al.*, 2017). This study found that the relative lumen number of cells was increased after RFA (Fig. 1F). Vascular permeability experiments found severe vascular leakage of HUVECs after HepG2-H incubation (Fig. 1G). In addition, the angiogenesis-related protein VEGFA was also detected and the finding indicated that VEGFA expression was elevated in HepG2-H cells after RFA (Fig. 1H). The above experiments manifested that RFA accelerated the growth of HCC cells and tumor angiogenesis.

Metformin restrains the growth and angiogenesis of HCC cells induced by RFA deficiency *in vitro*

To figure out whether metformin could mediate RFA deficiency-induced impacts on HCC cells, HCC cells were treated with metformin. Our data found that metformin inhibited the viability of HepG2 and HepG2-H cells and reduced colony numbers in a dose-dependent

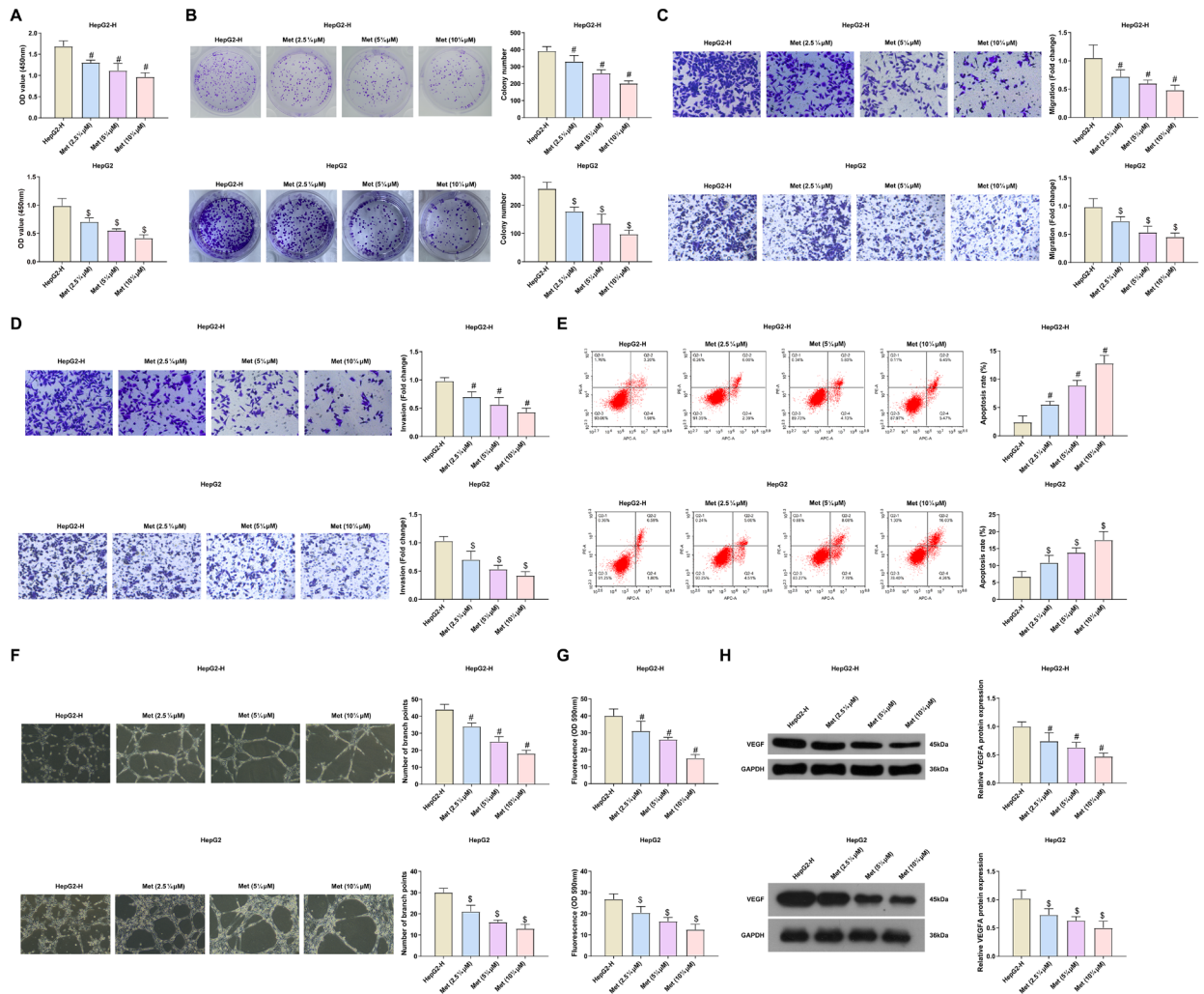


Figure 2. Metformin refrains the growth and angiogenesis of HCC cells induced by RFA deficiency *in vitro*

After metformin treatment, (A) CCK-8 detection of cell viability; (B) Plate clone detection of cell proliferation; (C/D) Transwell detection of cell migration and invasion; (E) Flow cytometry detection of cell apoptosis; (F) Detection of angiogenesis; (G) Permeability assay *in vitro*. (H) Western blot detection of angiogenesis-linked protein VEGFA. N=3. The measurement data were presented as mean \pm S.D. #vs. the HepG2-H, $P < 0.05$; vs. the HepG2, $P < 0.05$.

manner (Fig. 2A, B). RFA-induced quantitative increases in cell migration and invasion were also inhibited by metformin (Fig. 2C, D). Meanwhile, metformin also increased the apoptosis rate of HepG2 and HepG2-H cells in a dose-dependent manner (Fig. 2E) and inhibited tumor angiogenesis and permeability *in vitro* (Fig. 2F–H). All in all, metformin could refrain the growth and angiogenesis of HCC cells induced by RFA deficiency *in vitro*. The treatment effect of 10 μ M metformin was most pronounced and was therefore selected for further experiments.

MiR-302b-3p counteracts the therapeutic effect of metformin on RFA deficiency

Notably, miR-302b-3p levels were elevated in RFA-induced HepG2-H cells (Fig. 3A) which was dose-dependently counteracted by metformin (Fig. 3B). In addition, a decrease in miR-302b-3p expression was also detected in metformin-treated HepG2 cells (Fig. 3B). To further figure out miR-302b-3p's impacts on RFA deficiency, miR-302b-3p mimic and inhibitor were transfected in metformin-treated HepG2-H and HepG2 cells, and the

transfection efficiency was verified (Fig. 3C). Subsequent experiments manifested that miR-302b-3p mimic counteracted the therapeutic effects of metformin on HepG2-H and HepG2 cells, leading to promoted cell growth, angiogenesis, and vascular leakage, whereas miR-302b-3p inhibitor had the opposite effects (Fig. 3E–K).

MiR-302b-3p targets *TXNIP*

It was also found that *TXNIP* expression was reduced in RFA-induced HepG2-H cells (Fig. 4A, B), while metformin dose-dependently elevated *TXNIP* expression (Fig. 4C). TargetScan 7.2 predicted the binding site sequences of *TXNIP* and miR-302b-3p (Fig. 4E). The interaction between the two was further confirmed, clarifying that after co-transfection of the miR-302b-3p mimic with the psiCHECK-2 *TXNIP* 3'UTR Wt plasmid, the luciferase activity was reduced by 50% (Fig. 4F). It was further confirmed that miR-302b-3p could combine with *TXNIP* in RNA pull-down assay (Fig. 4G). In addition, the expression of miR-302b-3p and *TXNIP* in normal human liver cell line L02 and HepG2 cells was detected by PCR, and it was found that compared with L02, the

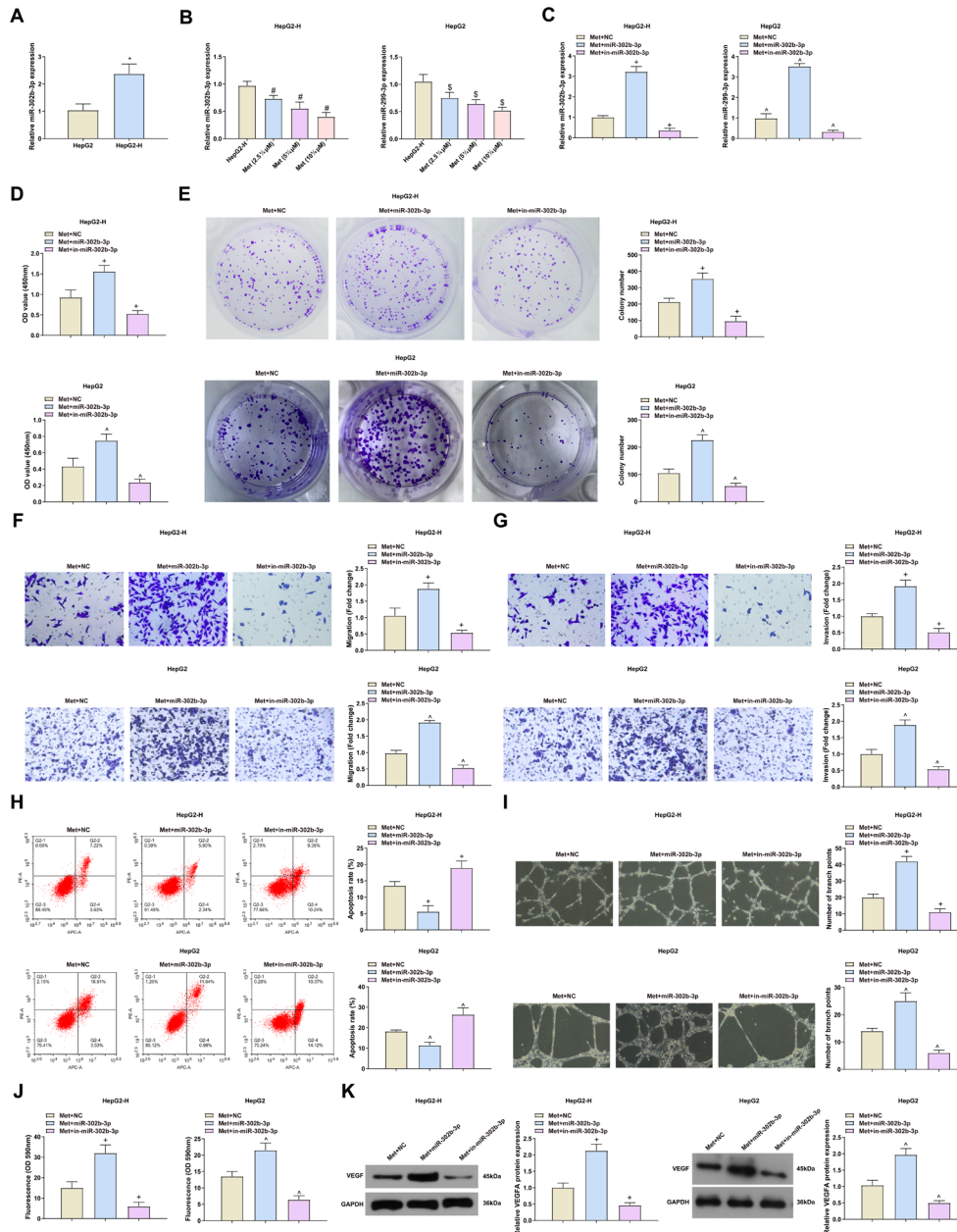


Figure 3. MIR-302b-3p counteracts the therapeutic effect of metformin on RFA deficiency

(A–C) PCR detection of miR-302b-3p; (D) CCK-8 detection of cell viability; (E) Plate clone detection of cell proliferation; (F/G) Transwell detection of cell migration and invasion; (H) Flow cytometry detection of cell apoptosis; (I) Detection of angiogenesis after metformin treatment; (J) Permeability assay *in vitro*. (K) Western blot detection of angiogenesis-linked protein VEGFA. N=3. The measurement data were presented as mean \pm S.D. *vs. the HepG2, $P < 0.05$; #vs. the HepG2-H, $P < 0.05$; + or ^vs. the Met+NC, $P < 0.05$.

expression of miR-302b-3p was increased, and the expression of *TXNIP* was decreased in HepG2 cells (Supplementary Fig. 1A,B). Next, *TXNIP* expression was measured in cells transfected with miR-302b-3p mimic or inhibitor, showing that miR-302b-3p mimic reduced *TXNIP*, while miR-302b-3p inhibitor elevated *TXNIP* expression (Supplementary Fig. 1C, Fig. 4HI at <https://ojs.ptbioch.edu.pl/i>). Taken together, miR-302b-3p could directly target *TXNIP*.

***TXNIP* turns around the effect of elevated miR-302b-3p on RFA-deficient HCC cells**

To further figure out the mechanism between *TXNIP* and miR-302b-3p, HepG2-H+Met cells or HepG2+Met

cells transfected with miR-302b-3p mimics were transfected with *TXNIP* overexpression vector (Fig. 5A). It was found that *TXNIP* reversed the effect of overexpression of miR-302b-3p on RFA-deficient HCC cells, reduced cell proliferation, migration, and invasion levels, increased apoptosis, and inhibited angiogenesis and permeability *in vitro* (Fig. 5B–I). In short, *TXNIP* turned around the effect of elevated miR-302b-3p on RFA-deficient HCC cells.

Metformin refrains RFA deficiency-induced HCC tumor growth and tumor vascular abnormalities *in vivo*

To figure out the application potential of metformin in the treatment of RFA deficiency *in vivo*, a residual can-

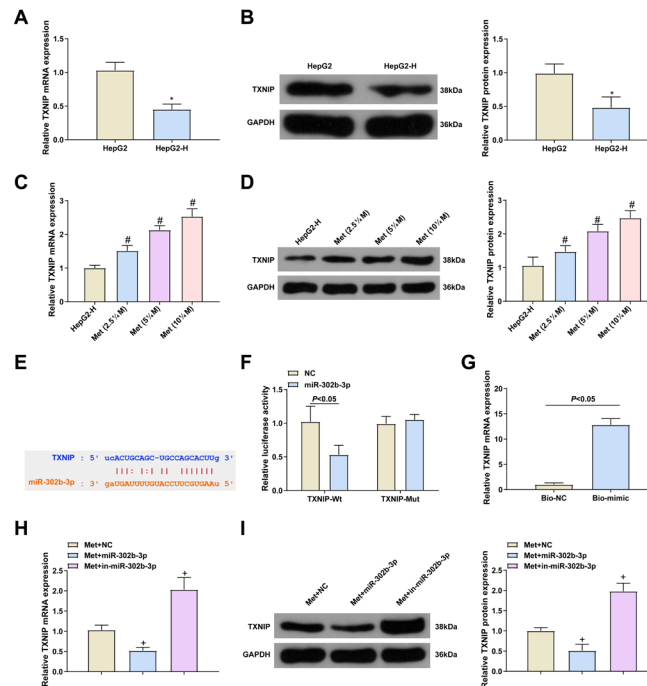


Figure 4. MiR-302b-3p targets TXNIP

(A–D) PCR and Western blot detection of *TXNIP* in cells; (E) TargetScan manifested the predicted *TXNIP* binding sequence of miR-302b-3p; (F) The luciferase activity assay in HepG2-H cells after co-transfection. (G) Enrichment of miR-302b-3p and *TXNIP* by RNA pull-down analysis; (H/I) PCR and Western blot detection of *TXNIP* in cells. N=3. The measurement data were presented as mean \pm S.D. *vs. the HepG2, $P<0.05$; #vs. the HepG2-H, $P<0.05$; +vs. the Met, $P<0.05$.

cer model of HCC after incomplete RFA was established in mice, and metformin was administered by gavage. It was discovered that tumor weight and volume were reduced in the HepG2-H+Met group (Fig. 6A–C). MiR-302b-3p and *TXNIP* expression in mouse tumor tissue was detected, manifesting that miR-302b-3p expression was reduced, but *TXNIP* expression was elevated in the HepG2-H+Met group (Fig. 6D, E). Moreover, microvessels were observed by CD31 staining and it was found that metformin reduced IMVD (Fig. 6F). Taken together, metformin repressed RFA-deficiency-induced HCC cell growth and tumor vascular abnormalities *in vivo*.

Up-regulation of miR-302b-3p enhances the malignancy of residual HCC cells after RFA

Finally, the correlation of miR-302b-3p with HCC development was analyzed. As shown in Fig. 7A, miR-302b-3p was elevated in HCC tissues compared with para-tumor tissues. More interestingly, miR-302b-3p was further enhanced in residual HCC tissues collected from RFA-deficient patients (Fig. 7B). These results suggest that miR-302b-3p may play an accelerating role in the development of residual HCC after RFA.

DISCUSSION

Angiogenesis has been reported to take on a critical role in the development, progression, and metastasis of HCC (Lin *et al.*, 2018). Many studies have testified that RFA is a safe and efficient approach for liver metastases, while residual tumors can grow aggressively after RFA, driven in part by the upregulation of VEGF (Agarwal *et al.*, 2014). Meanwhile, RFA deficiency promotes angiogenesis of residual HCC cells through HIF-1 α /VEGFA

axis (Kong *et al.*, 2012). These studies suggest that angiogenesis after RFA is a momentous physiological process in residual HCC. In the present study, it was found that RFA treatment accelerated HCC cell growth *in vitro*, increased cell relative lumen number, vascular permeability, and VEGFA expression. Metformin treatment could repress the facilitating effect of RFA on HCC. The *in vivo* results also confirmed that metformin could repress the growth and angiogenesis of HCC cells after RFA treatment.

It is well known that metformin is an anti-diabetic biguanide drug with safety and pleiotropic effects. In recent years, it has been proved to have anti-tumor effects in diversified cancers, such as cervical (Xia *et al.*, 2020), breast (Teufelsbauer *et al.*, 2020), and gastric cancers (Cunha Júnior *et al.*, 2021). Although some of the functions of metformin in HCC have been elucidated, many of its specific underlying mechanisms in HCC have not been identified, especially in HCC treated with RFA. In the study, RFA deficiency was simulated *in vitro* to construct a cell model, and it was found that RFA treatment facilitated HCC cell growth and angiogenesis, while metformin treatment restrained HCC cell growth, tumor angiogenesis, permeability, and VEGFA expression. Next, an RFA-deficient HCC *in vivo* model was established and administered metformin by gavage. It was discovered that metformin refrained RFA-deficiency-induced HCC cell growth and tumor vascular abnormalities *in vivo*, suggesting that metformin partially counteracts RFA deficiency-induced vascular abnormalities in HCC tumors. Some former studies have manifested that metformin represses tumorigenesis by modulating miRNAs. For example, metformin induces G1 cell cycle arrest by up-regulating tumor suppressors miR-let-7a, miR-let-7b, and miR-let-7e, thereby restraining HCC cell proliferation (Miyoshi *et al.*, 2014). Metformin stimulates pyroptosis

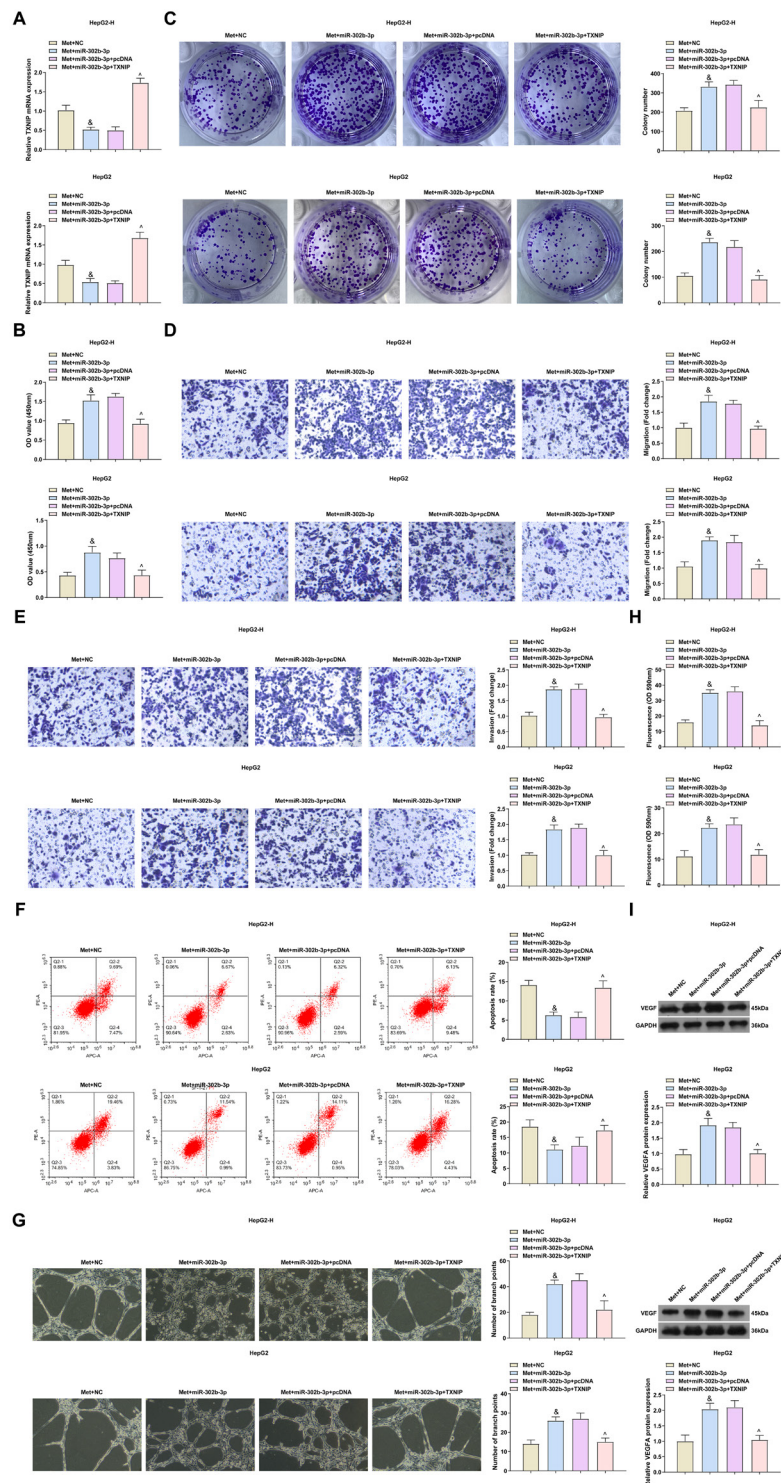


Figure 5. *TXNIP* turns around the effect of elevated miR-302b-3p on RFA-deficient HCC cells

(A) PCR detection of *TXNIP* in cells; (B) CCK-8 detection of cell viability; (C) Plate clone detection of cell proliferation; (D/E) Transwell detection of cell migration and invasion; (F) Flow cytometry detection of cell apoptosis; (G) Detection of angiogenesis after metformin treatment; (H) Permeability assay *in vitro*. (I) Western blot detection of angiogenesis-linked protein VEGFA. N=3. The measurement data were presented as mean \pm S.D. In HepG2-H cells, $^{\&}$ vs. the Met+NC, $^{\wedge}$ vs. the Met+miR-302b-3p+pcDNA, $P < 0.05$.

in human esophageal cancer cells by regulating miR-497 (Wang *et al.*, 2019). Here, it was discovered that metformin treatment downregulated miR-302b-3p in HCC.

Former studies have manifested that miR-302b-3p is abnormally expressed in diversified cancers (Liang *et al.*, 2019) and that it is also associated with nerve cell inflammation (He *et al.*, 2020) and neuronal damage (Li

et al., 2021). In this study, it was originally found that miR-302b-3p was elevated in RFA-induced HCC cells, and up-regulation of miR-302b-3p counteracted the therapeutic effect of metformin on HCC cells, while down-regulation of miR-302b-3p further enhanced the therapeutic effect of metformin on HCC. This result suggests miR-302b-3p was a downstream target of metformin in

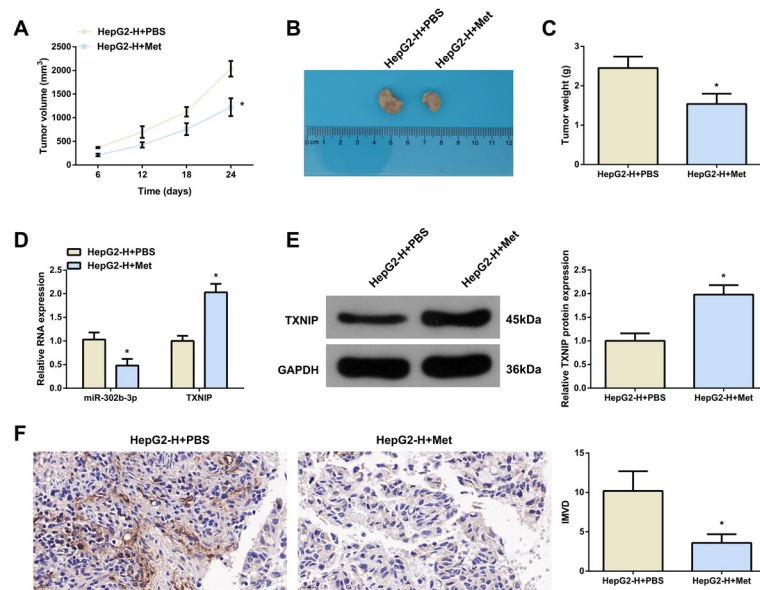
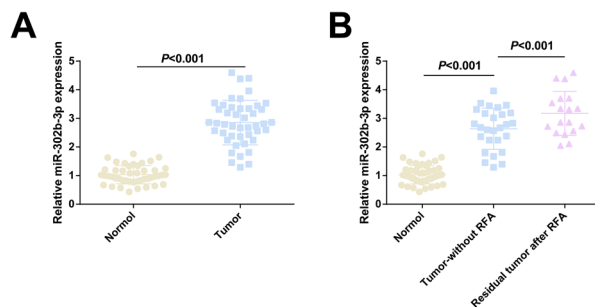


Figure 6. Metformin depresses RFA deficiency-induced HCC cell growth and tumor vascular abnormalities *in vivo* (A–C) Detection of the changes of tumor weight and volume in 30 d; (D/E) qPCR and Western Blot detection of miR-302b-3p and *TXNIP* in mouse tumor tissue; (F) CD31 staining to observe micro-vessels. $n=8$. The measurement data were presented as mean \pm S.D. *vs. the HepG2-H+PBS, $P<0.05$.



HCC. Many studies have manifested that miRNAs function in various diseases by targeting mRNAs. For example, miR-302b-3p targeting insulin-like growth factor 1 receptor represses gastric cancer cell proliferation (Guo *et al.*, 2017). Next, it was found that miR-302b-3p targeted *TXNIP* in RFA-induced HCC cells. TargetScan 7.2 forecasted the existence of binding sites for miR-302b-3p and *TXNIP*.

TXNIP is an α -arrest family protein that modulates intracellular reactive oxygen species (ROS) (Sheth *et al.*, 2006). *TXNIP* takes on an irreplaceable role in the development of HCC, and *TXNIP* deficiency is sufficient to induce HCC and *TXNIP* is a new tumor suppressor gene for HCC (Sheth *et al.*, 2006). In the present study, it was found that *TXNIP* was down-regulated in RFA-induced HCC cells, and elevation of *TXNIP* turned around the effect of elevated miR-302b-3p on RFA-deficient HCC and refrained HCC cell growth, angiogenesis, and permeability *in vitro*. These results suggested that metformin repressed HCC cell growth and angiogenesis *in vitro* and *in vivo* by targeting the miR-302b-3p/*TXNIP* axis.

However, the research still has some limitations. First, the sample size was insufficient due to limited laboratory conditions. Meanwhile, it has been documented that ROS production is elevated after RFA (Richter *et*

al., 2012), while the effect of RFA deficiency on ROS production and whether ROS in turn affects HCC cell growth and angiogenesis remains to be further verified. It is hoped that these issues can be further addressed.

CONCLUSION

Overall, the study manifests that RFA deficiency can accelerate cell growth and angiogenesis in HCC, while metformin can alleviate the negative impact of RFA deficiency on HCC. The results suggest that metformin represses HCC cell growth and angiogenesis *in vitro* and *in vivo* by miR-302b-3p to upregulate *TXNIP*. The results offer brand-new insights into overcoming RFA deficiency to promote the malignant progression of residual HCC cells.

Declarations

Acknowledgments. Not applicable.

Ethics Statement. All procedures and animal care were approved by Beijing Chaoyang Hospital Affiliated to Capital Medical University of Science and Technology Animal Care Committee and performed according to NIH guidelines. Ethics approval number: BJ2018TJSJ2203.

Funding. Not applicable

Declaration of Conflicting Interests. Authors declared no conflict of interest.

REFERENCES

- Agarwal A, Daly KP, Butler-Bowen H, Saif MW (2014) Safety and efficacy of radiofrequency ablation with aflibercept and FOLFIRI in a patient with metastatic colorectal cancer. *Anticancer Res* **34**: 6775–6778
- Alberti C, Manzenreither RA, Sowemimo I, Burkard TR, Wang J, Mahofsky K, Ameres SL, Cochella L (2018) Cell-type specific sequencing of microRNAs from complex animal tissues. *Nat Methods* **15**: 283–289. <https://doi.org/10.1038/nmeth.4610>

- Cunha Júnior AD, Bragagnoli AC, Costa FO, Carvalheira JBC (2021) Repurposing metformin for the treatment of gastrointestinal cancer. *World J Gastroenterol* **27**: 1883–1904. <https://doi.org/10.3748/wjg.v27.i17.1883>
- El Shorbagy S, abuTaleb F, Labib HA, Ebian H, Harb OA, Mohammed MS, Rashied HA, Elbana KA, Haggag R (2021) Prognostic significance of VEGF and HIF-1 α in hepatocellular carcinoma patients receiving sorafenib versus metformin sorafenib combination. *J Gastrointest Cancer* **52**: 269–279. <https://doi.org/10.1007/s12029-020-00389-w>
- Guo B, Zhao Z, Wang Z, Li Q, Wang X, Wang W, Song T, Huang C (2017) MicroRNA-302b-3p suppresses cell proliferation through AKT pathway by targeting IGF-1R in human gastric cancer. *Cell Physiol Biochem* **42**: 1701–1711. <https://doi.org/10.1159/000479419>
- Harati R, Vandamme M, Blanchet B, Bardin C, Praz F, Hamoudi RA, Desbois-Mouthon C (2021) Drug-drug interaction between metformin and sorafenib alters antitumor effect in hepatocellular carcinoma cells. *Mol Pharmacol* **100**: 32–45. <https://doi.org/10.1124/molpharm.120.000223>
- He Q, Li Y, Zhang W, Chen J, Deng W, Liu Q, Liu Y, Liu D (2021) Role and mechanism of TXNIP in ageing-related renal fibrosis. *Mech Ageing Dev* **196**: 111475. <https://doi.org/10.1016/j.mad.2021.111475>
- He R, Tang GL, Niu L, Ge C, Zhang XQ, Ji XF, Fang H, Luo LZ, Chen M, Shang XF (2020) Quietness Circ 0009062 promoted nerve cell inflammation through PIK3CA/Akt/NF- κ B signaling by miR-302b-3p in spinal cord injury. *Ann Palliat Med* **9**: 190–198. <https://doi.org/10.21037/apm.2020.02.13>
- Hu F, Li M, Mo L, Xiao Y, Wang X, Xie B (2021) SOX-17 is involved in invasion and apoptosis of colorectal cancer cells through regulating miR-302b-3p expression. *Cell Biol Int* **45**: 1296–1305. <https://doi.org/10.1002/cbin.11594>
- Hu L, Zeng Z, Xia Q, Liu Z, Feng X, Chen J, Huang M, Chen L, Fang Z, Liu Q, Zeng H, Zhou X, Liu J (2019) Metformin attenuates hepatoma cell proliferation by decreasing glycolytic flux through the HIF-1 α /PFKFB3/PFK1 pathway. *Life Sci* **239**: 116966. <https://doi.org/10.1016/j.lfs.2019.116966>
- Jia G, Li F, Tong R, Liu Y, Zuo M, Ma L, Ji X (2020) c-Met/MAPK pathway promotes the malignant progression of residual hepatocellular carcinoma cells after insufficient radiofrequency ablation. *Med Oncol* **37**: 117. <https://doi.org/10.1007/s12032-020-01444-z>
- Jiang C, He ZL, Hu XH, Ma PY (2020) MiRNA-15a-3p inhibits the metastasis of hepatocellular carcinoma by interacting with HMOX1. *Eur Rev Med Pharmacol Sci* **24**: 12694–12700. https://doi.org/10.26355/eurrev_202012_24167
- Kong J, Kong J, Pan B, Ke S, Dong S, Li X, Zhou A, Zheng L, Sun WB (2012) Insufficient radiofrequency ablation promotes angiogenesis of residual hepatocellular carcinoma via HIF-1 α /VEGFA. *PLoS One* **7**: e37266. <https://doi.org/10.1371/journal.pone.0037266>
- Lassandro G, Picchi SG, Bianco A, Di Costanzo G, Coppola A, Ierardi AM, Lassandro F (2020) Effectiveness and safety in radiofrequency ablation of pulmonary metastases from HCC: a five years study. *Med Oncol* **37**: 25. <https://doi.org/10.1007/s12032-020-01352-2>
- Li L, Lu S, Fan X (2021) Silencing of miR-302b-3p alleviates isoflurane-induced neuronal injury by regulating PTEN expression and AKT pathway. *Brain Res Bull* **168**: 89–99. <https://doi.org/10.1016/j.brainresbull.2020.12.016>
- Liao ZB, Tan XL, Dong KS, Zhang HW, Chen XP, Chu L, Zhang BX (2019, May) miRNA-448 inhibits cell growth by targeting BCL-2 in hepatocellular carcinoma. *Dig Liver Dis* **51**: 703–711. <https://doi.org/10.1016/j.dld.2018.09.021>
- Lin J, Cao S, Wang Y, Hu Y, Liu H, Li J, Chen J, Li P, Liu J, Wang Q, Zheng L (2018) Long non-coding RNA UBE2CP3 enhances HCC cell secretion of VEGFA and promotes angiogenesis by activating ERK1/2/HIF-1 α /VEGFA signalling in hepatocellular carcinoma. *J Exp Clin Cancer Res* **37**: 113. <https://doi.org/10.1186/s13046-018-0727-1>
- Miyoshi H, Kato K, Iwama H, Maeda E, Masaki T (2014) Effect of the anti-diabetic drug metformin in hepatocellular carcinoma *in vitro* and *in vivo*. *Int J Oncol* **45**: 322–332. <https://doi.org/10.3892/ijo.2014.2419>
- Ni C, Yang S, Ji Y, Duan Y, Yang W, Yang X, Li M, Xie J, Zhang C, Lu Y, Lu H (2021) Hsa_circ_0011385 knockdown represses cell proliferation in hepatocellular carcinoma. *Cell Death Discov* **7**: 270. <https://doi.org/10.1038/s41420-021-00664-0>
- Ramjiawan RR, Griffioen AW, Duda DG (2017) Anti-angiogenesis for cancer revisited: Is there a role for combinations with immunotherapy? *Angiogenesis* **20**: 185–204. <https://doi.org/10.1007/s10456-017-9552-y>
- Richter B, Gwechenberger M, Socas A, Zorn G, Albinni S, Marx M, Bergler-Klein J, Binder T, Wojta J, Gössinger HD (2012) Markers of oxidative stress after ablation of atrial fibrillation are associated with inflammation, delivered radiofrequency energy and early recurrence of atrial fibrillation. *Clin Res Cardiol* **101**: 217–225. <https://doi.org/10.1007/s00392-011-0383-3>
- Schulte L, Scheiner B, Voigtländer T, Koch S, Schweitzer N, Marhenke S, Ivanyi P, Manns MP, Rodt T, Hinrichs JB, Weinmann A, Pinter M, Vogel A, Kirstein MM (2019) Treatment with metformin is associated with a prolonged survival in patients with hepatocellular carcinoma. *Liver Int* **39**: 714–726. <https://doi.org/10.1111/liv.14048>
- Shankaraiah RC, Callegari E, Guerriero P, Rimessi A, Pinton P, Gramantieri L, Silini EM, Sabbioni S, Negrini M (2019) Metformin prevents liver tumourigenesis by attenuating fibrosis in a transgenic mouse model of hepatocellular carcinoma. *Oncogene* **38**: 7035–7045. <https://doi.org/10.1038/s41388-019-0942-z>
- Sheth SS, Bodnar JS, Ghazalpour A, Thippavong CK, Tsutsumi S, Tward AD, Demant P, Kodama T, Aburatani H, Lusis AJ (2006) Hepatocellular carcinoma in Txnip-deficient mice. *Oncogene* **25**: 3528–3536. <https://doi.org/10.1038/sj.onc.1209394>
- Sun Y, Liu L, Xing W, Sun H (2021) microRNA-148a-3p enhances the effects of sevoflurane on hepatocellular carcinoma cell progression via ROCK1 repression. *Cell Signal* **83**: 109982. <https://doi.org/10.1016/j.cellsig.2021.109982>
- Teng F, Zhang JX, Chang QM, Wu XB, Tang WG, Wang JF, Feng JF, Zhang ZP, Hu ZQ (2020) LncRNA MYLK-AS1 facilitates tumor progression and angiogenesis by targeting miR-424-5p/E2F7 axis and activating VEGFR-2 signaling pathway in hepatocellular carcinoma. *J Exp Clin Cancer Res* **39**: 235. <https://doi.org/10.1186/s13046-020-01739-z>
- Teufelsbauer M, Rath B, Plangger A, Staud C, Nanobashvili J, Huk I, Neumayer C, Hamilton G, Radtke C (2020) Effects of metformin on adipose-derived stromal cell (ADSC) – Breast cancer cell lines interaction. *Life Sci* **261**: 118371. <https://doi.org/10.1016/j.lfs.2020.118371>
- Wang D, Jiang X, Liu Y, Cao G, Zhang X, Kuang Y (2021) Circular RNA circ_HN1 facilitates gastric cancer progression through modulation of the miR-302b-3p/ROCK2 axis. *Mol Cell Biochem* **476**: 199–212. <https://doi.org/10.1007/s11010-020-03897-2>
- Wang L, Li K, Lin X, Yao Z, Wang S, Xiong X, Ning Z, Wang J, Xu X, Jiang Y, Liu D, Chen Y, Zhang D, Zhang H (2019) Metformin induces human esophageal carcinoma cell pyroptosis by targeting the miR-497/PELP1 axis. *Cancer Lett* **450**: 22–31. <https://doi.org/10.1016/j.canlet.2019.02.014>
- Xia C, Liu C, He Z, Cai Y, Chen J (2020) Metformin inhibits cervical cancer cell proliferation by modulating PI3K/Akt-induced major histocompatibility complex class I-related chain A gene expression. *J Exp Clin Cancer Res* **39**: 127. <https://doi.org/10.1186/s13046-020-01627-6>
- Xu G, Zhang P, Liang H, Xu Y, Shen J, Wang W, Li M, Huang J, Ni C, Zhang X, Zhu X (2021) Circular RNA hsa_circ_0003288 induces EMT and invasion by regulating hsa_circ_0003288/miR-145/PD-L1 axis in hepatocellular carcinoma. *Cancer Cell Int* **21**: 212. <https://doi.org/10.1186/s12935-021-01902-2>
- Xu H, Miao X, Li X, Chen H, Zhang B, Zhou W (2021) LncRNA SNHG16 contributes to tumor progression via the miR-302b-3p/SLC2A4 axis in pancreatic adenocarcinoma. *Cancer Cell Int* **21**: 51. <https://doi.org/10.1186/s12935-020-01715-9>
- Yerukala Sathipati S, Ho SY (2020) Novel miRNA signature for predicting the stage of hepatocellular carcinoma. *Sci Rep* **10**: 14452. <https://doi.org/10.1038/s41598-020-71324-z>
- You A, Cao M, Guo Z, Zuo B, Gao J, Zhou H, Li H, Cui Y, Fang F, Zhang W, Song T, Li Q, Zhu X, Yin H, Sun H, Zhang T (2016) Metformin sensitizes sorafenib to inhibit postoperative recurrence and metastasis of hepatocellular carcinoma in orthotopic mouse models. *J Hematol Oncol* **9**: 20. <https://doi.org/10.1186/s13045-016-0253-6>
- Yuan Z, Ye M, Qie J, Ye T (2020) FOXA1 Promotes cell proliferation and suppresses apoptosis in HCC by directly regulating miR-212-3p/FOXA1/AGR2 signaling pathway. *Oncol Targets Ther* **13**: 5231–5240. <https://doi.org/10.2147/ott.s252890>
- Zhang HH, Zhang Y, Cheng YN, Gong FL, Cao ZQ, Yu LG, Guo XL (2018) Metformin in combination with curcumin inhibits the growth, metastasis, and angiogenesis of hepatocellular carcinoma *in vitro* and *in vivo*. *Mol Carcinog* **57**: 44–56. <https://doi.org/10.1002/mc.22718>
- Zhang Q, Kong J, Dong S, Xu W, Sun W (2017) Metformin exhibits the anti-proliferation and anti-invasion effects in hepatocellular carcinoma cells after insufficient radiofrequency ablation. *Cancer Cell Int* **17**: 48. <https://doi.org/10.1186/s12935-017-0418-6>
- Zhang Y, Zhang H, Wu S (2021) LncRNA-CCDC144NL-AS1 Promotes the development of hepatocellular carcinoma by inducing WDR5 expression via sponging miR-940. *J Hepatocell Carcinoma* **8**: 333–348. <https://doi.org/10.2147/jhc.s306484>
- Zhao D, Xia L, Geng W, Xu D, Zhong C, Zhang J, Xia Q (2021) Metformin suppresses interleukin-22 induced hepatocellular carcinoma by upregulating Hippo signaling pathway. *J Gastroenterol Hepatol* **36**: 3469–3476. <https://doi.org/10.1111/jgh.15674>
- Zhu L, Yang N, Li C, Liu G, Pan W, Li X (2019) Long noncoding RNA NEAT1 promotes cell proliferation, migration, and invasion in hepatocellular carcinoma through interacting with miR-384. *J Cell Biochem* **120**: 1997–2006. <https://doi.org/10.1002/jcb.27499>